

# Unsaturation in homoleptic tetranuclear iridium carbonyls: a comparison of density functional theory with the MP2 method in metal cluster structures

Qing Kui Chi · Qian-shu Li · Yaoming Xie ·  
R. Bruce King · Henry F. Schaefer III

Received: 22 February 2011 / Accepted: 14 July 2011 / Published online: 6 August 2011  
© Springer-Verlag 2011

**Abstract** The lowest energy  $\text{Ir}_4(\text{CO})_{12}$  structure is predicted by density functional theory to be a triply bridged structure analogous to the experimental structures for its lighter congeners  $\text{M}_4(\text{CO})_9(\mu\text{-CO})_3$  ( $\text{M}=\text{Co}, \text{Rh}$ ). The experimental unbridged structure for  $\text{Ir}_4(\text{CO})_{12}$  is predicted to lie  $\sim 6$  kcal/mol above the triply bridged structure. However, the MP2 method predicts the unbridged structure for  $\text{Ir}_4(\text{CO})_{12}$  to be the lowest energy structure by  $\sim 9$  kcal/mol over the triply bridged structure. The lowest energy  $\text{Ir}_4(\text{CO})_{11}$  structure is predicted to be a doubly bridged structure with a central tetrahedral  $\text{Ir}_4$  unit. A higher energy  $\text{Ir}_4(\text{CO})_{11}$  structure at  $\sim 18$  kcal/mol above this global minimum is found with an unusual  $\mu_4\text{-CO}$  group bridging all four atoms of a central  $\text{Ir}_4$  butterfly. This  $\text{Ir}_4(\text{CO})_8(\mu\text{-CO})_2(\mu_4\text{-CO})$  structure is analogous to the lowest energy

$\text{Co}_4(\text{CO})_{11}$  structure found in a previous theoretical study, as well as  $\text{Rh}_4(\text{CO})_4(\mu\text{-CO})_4(\text{PBu}_3^t)_2(\text{PtPBu}_3^t)(\mu_4\text{-CO})$ , which has been synthesized by Adams and coworkers. The  $\text{Ir}_4$  tetrahedron is remarkably persistent in the more highly unsaturated  $\text{Ir}_4(\text{CO})_n$  ( $n = 10, 9, 8$ ) structures with relatively little changes in the Ir–Ir distances as carbonyl groups are removed. This appears to be related to the spherical aromaticity in the tetrahedral  $\text{Ir}_4$  structures.

**Keywords** Iridium · Metal carbonyls · Metal clusters · Density functional theory · Møller–Plesset second-order perturbation theory

## 1 Introduction

The chemistry of homoleptic iridium carbonyls dates back to 1940 when Hieber and Lagally [1] first reported the synthesis of  $\text{Ir}_4(\text{CO})_{12}$  by the reaction of anhydrous iridium halides with carbon monoxide at elevated temperatures and pressures in the presence of copper or silver as a halogen acceptor. Several improvements in this original synthesis of  $\text{Ir}_4(\text{CO})_{12}$  have subsequently been reported providing higher yields and/or allowing milder reaction conditions [2–5]. Furthermore,  $\text{Ir}_4(\text{CO})_{12}$  is one of the most stable and least reactive of the known saturated homoleptic metal carbonyls.

Determination of the structure of  $\text{Ir}_4(\text{CO})_{12}$  by X-ray crystallography for some time was very difficult because of disorder problems [6]. However, the structure of  $\text{Ir}_4(\text{CO})_{12}$  clearly consists of a central  $\text{Ir}_4$  tetrahedron with three terminal carbonyl groups on each iridium atom. The absence of bridging carbonyl groups in  $\text{Ir}_4(\text{CO})_{12}$  is also confirmed by the  $\nu(\text{CO})$  infrared spectrum, which shows only terminal carbonyl groups. This  $\text{Ir}_4(\text{CO})_{12}$  structure differs from the structures of the corresponding cobalt and rhodium

Dedicated to Professor Shigeru Nagase on the occasion of his 65th birthday and published as part of the Nagase Festschrift Issue.

**Electronic supplementary material** The online version of this article (doi:10.1007/s00214-011-1005-x) contains supplementary material, which is available to authorized users.

Q. K. Chi · Q. Li (✉) · R. B. King (✉)  
Center for Computational Quantum Chemistry,  
South China Normal University, Guangzhou 510631,  
People's Republic of China  
e-mail: qqli@scnu.edu.cn

R. B. King  
e-mail: rbking@chem.uga.edu

Q. Li  
Institute of Chemical Physics, Beijing Institute of Technology,  
Beijing 100081, People's Republic of China

Y. Xie · R. B. King · H. F. Schaefer III  
Department of Chemistry and Center for Computational  
Chemistry, University of Georgia, Athens, GA 30602, USA

derivatives  $M_4(CO)_{12}$  ( $M=Co$  [7],  $Rh$  [8, 9]), in which the three edges of one of the  $M_3$  triangular faces of the central  $M_4$  tetrahedron are bridged by carbonyl groups, leaving nine terminal carbonyl groups (Fig. 1).

The central  $Ir_4$  tetrahedron in  $Ir_4(CO)_{12}$  is sufficiently favored that it is preserved in many reactions of  $Ir_4(CO)_{12}$ , such as those with bases of various types [10]. This suggests that the prospects of synthesizing or generating unsaturated tetranuclear  $Ir_4(CO)_n$  ( $n = 11, 10, 9,$  and  $8$ ) derivatives by removal of one or more carbonyl groups, possibly in low temperature matrices, are better than with those of the lighter congeners  $M_4(CO)_{12}$  ( $M=Co, Rh$ ), where the  $M-M$  bonds in the central  $M_4$  tetrahedra are more susceptible to rupture. Furthermore, the  $M_4(CO)_{11}$  systems are of interest since in the lowest energy  $Co_4(CO)_{11}$  structure a  $Co-Co$  edge breaks to form a central  $Co_4$  butterfly that is bridged by an unusual  $\mu_4-CO$  group bonded to all four cobalt atoms (Fig. 2) [11]. Homoleptic metal carbonyl clusters with  $\mu_4-CO$  groups bridging four metal atoms have not been synthesized. However, a  $\mu_4-CO$  group is found in the related compound  $Rh_4(CO)_4(\mu-CO)_4(PBu_3)_2(PtPBu_3)(\mu_4-CO)$ , which has been synthesized by Adams and coworkers [12]. The latter structure can be considered as a substitution product of  $Rh_4(CO)_{10}(\mu_4-CO)$  in which two carbonyl groups are replaced by tertiary

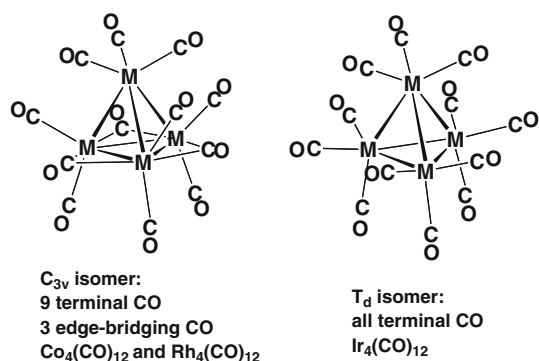


**Fig. 1** A comparison of the triply bridged structures of  $M_4(CO)_{12}$  ( $M=Co, Rh$ ) with the unbridged structure of  $Ir_4(CO)_{12}$

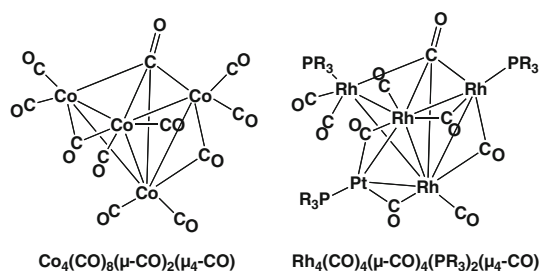


**Fig. 2** A comparison of the structures of  $Co_4(CO)_8(\mu-CO)_2(\mu_4-CO)$  and  $Rh_4(CO)_4(\mu-CO)_4(PBu_3)_2(PtPBu_3)(\mu_4-CO)$

phosphines and a third carbonyl group by a two-electron donor  $R_3PPt(CO)$  unit.

This paper reports a theoretical study of  $Ir_4(CO)_n$  ( $n = 12, 11, 10, 9,$  and  $8$ ) derivatives using density functional theory methods shown in previous work to be reliable for various osmium carbonyl derivatives including trinuclear [13] and tetranuclear [14] clusters. A major objective of this work was to search for structures with unusual carbonyl groups, either bridging three or four atoms or functioning as four-electron  $\eta^2-\mu-CO$  donors. Also of special interest are unsaturated  $Ir_4(CO)_n$  structures with unusually short  $Ir-Ir$  distances suggestive of formal multiple bonding.

## 2 Theoretical methods

Density functional theory methods (DFT) have been acknowledged to be a practical and effective tool for the computation of organometallic compounds [15–21]. Two DFT methods, namely BP86, and MPW1PW91, were used in this study. The BP86 method is a pure DFT method that combines Becke's 1988 exchange functional with Perdew's 1986 correlation functional [22, 23]. The MPW1PW91 method [24], based on the generalized gradient approximation (GGA) is a newer density functional and may be more suitable for the second and third row transition metal systems [25]. In order to gauge the reliability of the relative energies obtained by these DFT methods, single-point energies were obtained using the Møller–Plesset second-order perturbation theory (MP2) method [26, 27] at the optimized MPW1PW91 geometries.

For the third row transition metals, the large numbers of electrons increase exponentially the computational efforts. In order to reduce the cost, effective core potential (ECP) relativistic basis sets are employed. The Stuttgart relativistic small-core (SRSC) double- $\zeta$  basis set with an effective core potential (ECP) [28, 29] was used for the iridium atoms. In this basis set, the electrons in the lowest 28 spin-orbitals (1s to 3d) for the iridium atoms are replaced by an effective core potential (ECP), and the valence basis set is contracted from (8s7p6d) primitive sets to (6s5p3d). The effective core approximation includes scalar relativistic contributions, which may become significant for the heavy transition metal atoms. For the carbon and oxygen the double- $\zeta$  plus polarization (DZP) basis sets, which add one set of pure spherical harmonic d functions with orbital exponents  $\alpha_d(C) = 0.75$  and  $\alpha_d(O) = 0.85$  to the Huzinaga–Dunning standard contracted DZ sets [30, 31], are used and designated (9s5p1d/4s2p1d). The basis set for carbon and oxygen with the pure spherical harmonic d functions used in this work is larger than the (9s5p/4s/2p) basis set used in the previous work [13] on  $Os_3(CO)_n$  ( $n = 12, 11, 10, 9$ ), which did not include the d functions.

The geometries of all structures were fully optimized using the DFT methods (BP86, and MPW1PW91) along with the ECP (SDD) basis sets. The vibrational frequencies were determined by evaluating analytically the second derivatives of the energy with respect to the nuclear coordinates at the same levels. The corresponding infrared intensities were also evaluated analytically. All of the computations were carried out with the Gaussian 03 program [32], in which the (75, 302) grid is the default for evaluating integrals numerically [33]. The finer (120, 974) grid for evaluating integrals numerically is used for evaluating the imaginary vibrational frequencies [33], while the tight ( $10^{-8}$  hartree) designation is the default for the self-consistent field (SCF) convergence. In all cases, triplet  $\text{Ir}_4(\text{CO})_n$  structures were found to have higher energies than corresponding singlet structures. Therefore, only singlet structures are discussed in this paper.

The optimized structures are depicted in Figs. 3, 4, 5, 6. In these figures, the top distance labels refer to results obtained by the BP86 method and the bottom distance labels refer to the MPW1PW91 predictions. A given structure is designated **a**, **b**, where **a** is the number of CO groups and **b** orders the structures according to their relative energies. Thus, the lowest energy structure of  $\text{Ir}_4(\text{CO})_{12}$  is designated **12-1**.

### 3 Results and discussion

#### 3.1 Molecular structures

A total of 17 structures for the neutral tetranuclear derivatives  $\text{Ir}_4(\text{CO})_n$  ( $n = 12, 11, 10, 9$ , and 8) were fully optimized in this work. The structures within  $\sim 25$  kcal/mol of the global minima are discussed here. The theoretical harmonic  $\nu(\text{CO})$  frequencies using the BP86/SDD method are listed in the tables in the present paper, since methods based on the BP86 functional are generally more reliable for predicting  $\nu(\text{CO})$  frequencies than those based on the MPW1PW91 functional [34, 35]. In addition, the energies and geometries for the  $\text{Ir}_4(\text{CO})_n$  ( $n = 12, 11, 10, 9$ , and 8) structures predicted by the MPW1PW91/SDD and BP86/SDD methods are discussed specifically in this paper.

##### 3.1.1 $\text{Ir}_4(\text{CO})_{12}$

The lowest energy structure predicted by the DFT methods for  $\text{Ir}_4(\text{CO})_{12}$  is a triply bridged  $C_{3v}$  tetrahedral structure **12-1** rather than the experimentally known [6] unbridged structure **12-2** (Fig. 3). However, the MP2 method predicts the global minimum to be the unbridged structure **12-2** (Fig. 3), lying  $\sim 9$  kcal/mol below **12-1**. The  $\text{Ir}_4(\text{CO})_{12}$  structure **12-1** has three carbonyl groups bridging the edges of a triangular face

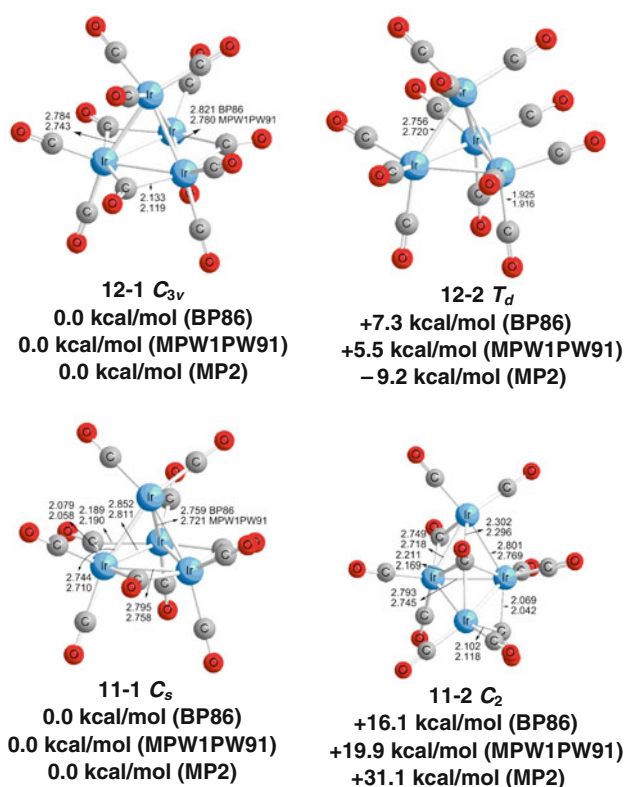


Fig. 3 The optimized structures for  $\text{Ir}_4(\text{CO})_{12}$  and  $\text{Ir}_4(\text{CO})_{11}$

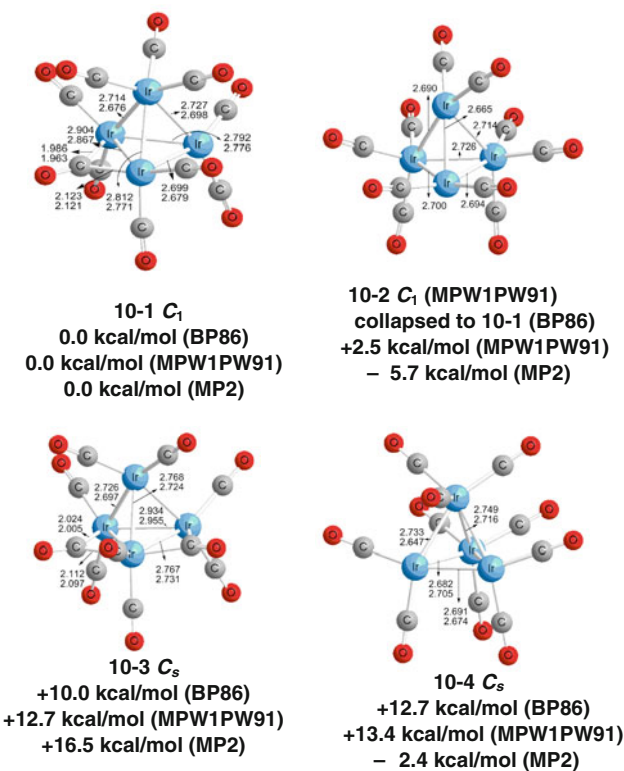
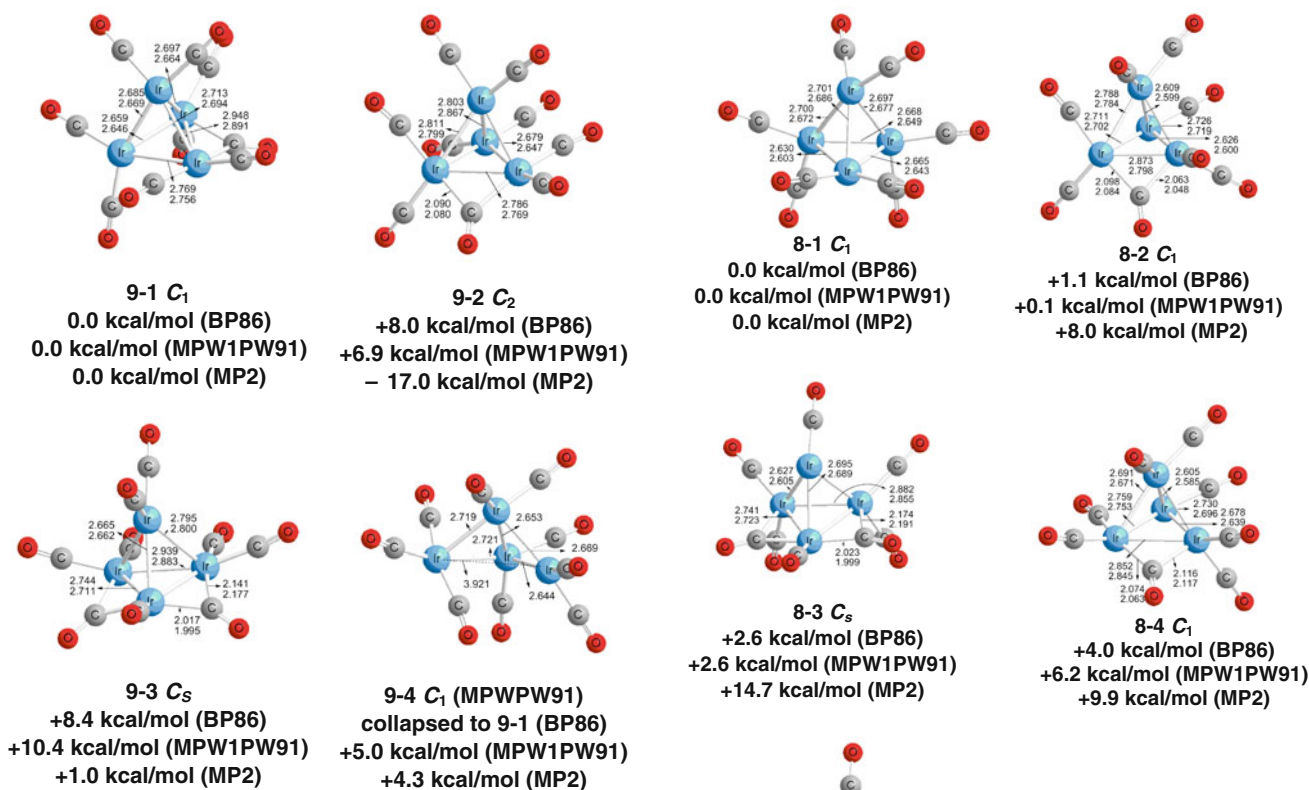


Fig. 4 The optimized structures for  $\text{Ir}_4(\text{CO})_{10}$



**Fig. 5** The optimized structures for Ir<sub>4</sub>(CO)<sub>9</sub>

of the Ir<sub>4</sub> tetrahedron. The remaining nine carbonyl groups in **12-1** are all terminal groups with two on each of the three iridium atoms connected to the CO-bridged edges and three on the iridium atom not connected to any of the bridged edges. This structure is analogous to the structures of the lighter congeners Co<sub>4</sub>(CO)<sub>12</sub> and Rh<sub>4</sub>(CO)<sub>12</sub>, determined by X-ray crystallography [7, 8, 36]. The bridging CO groups in Ir<sub>4</sub>(CO)<sub>12</sub> are predicted to exhibit a weak band at 1,892 cm<sup>−1</sup> and a much stronger band at 1,864 cm<sup>−1</sup> in the usual bridging ν(CO) region (Table 1). In **12-1** the CO-bridged Ir–Ir edge lengths are 2.821 Å (BP86) or 2.780 Å (MPW1PW91) and the unbridged Ir–Ir edge lengths are 2.784 Å (BP86) or 2.743 Å (MPW1PW91).

The second Ir<sub>4</sub>(CO)<sub>12</sub> structure is a T<sub>d</sub> tetrahedral structure **12-2**, lying either 7.3 kcal/mol (BP86) or 5.5 kcal/mol in energy (MPW1PW91) above the global minimum **12-1** or 9.2 kcal/mol below **12-1** (MP2). Structure **12-2** rather than **12-1** is the structure found experimentally for Ir<sub>4</sub>(CO)<sub>12</sub> by X-ray crystallography [6]. The six equivalent Ir–Ir distances in **12-2** are predicted to be 2.756 Å (BP86) or 2.720 Å (MPW1PW91). The MPW1PW91 method thus predicts Ir–Ir distances in **12-2** closer to the experimental value of 2.693 Å than the BP86 method. This is consistent with a previous theoretical study [25] on second row transition metal carbonyls such as Mo(CO)<sub>6</sub> and Ru<sub>3</sub>(CO)<sub>12</sub>.

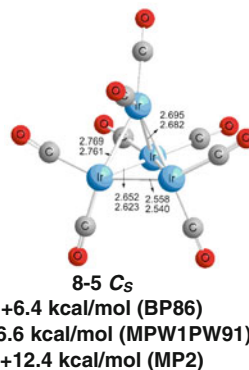


**Fig. 6** The optimized structures for Ir<sub>4</sub>(CO)<sub>8</sub>

### 3.1.2 Ir<sub>4</sub>(CO)<sub>11</sub>

By analogy to Ir<sub>4</sub>(CO)<sub>12</sub> discussed above, we tried to optimize triply bridged and unbridged structures of Ir<sub>4</sub>(CO)<sub>11</sub>. This search led to two structures, namely **11-1** and **11-2** (Fig. 3). The C<sub>s</sub> structure for Ir<sub>4</sub>(CO)<sub>11</sub>, namely **11-1** (Fig. 3), is a triply bridged structure, which can be derived from **12-1** by loss of a CO group from the unique Ir(CO)<sub>3</sub> moiety. The four independent Ir–Ir lengths in **11-1** are predicted by the MPW1PW91 method to be 2.710, 2.721, 2.758, and 2.811 Å, which are very similar to those in **12-1** and the Ir–Ir distance of 2.693 Å found from crystallography for **12-2**. This suggests that the Ir–Ir bonds remain formal single bonds upon loss of a CO group from **12-1** with one iridium atom losing a CO group thereby going from a favorable 18-electron configuration to an unsaturated 16-electron configuration.

**Table 1** Infrared  $\nu(\text{CO})$  vibrational frequencies ( $\text{cm}^{-1}$ ) predicted for the  $\text{Ir}_4(\text{CO})_{12}$  and  $\text{Ir}_4(\text{CO})_{11}$  structures

<b>12-1</b>	<b>1864(749), 1864(749), 1892(2)</b> , 1995(117), 1995(117), 2009(265), 2009(265), 2014(691), 2043(1436), 2043(1436), 2043(1836), 2075(1)
<b>12-2</b>	1978(0), 1978(0), 1978(0), 1991(0), 1991(0), 2007(252), 2007(252), 2007(252), 2042(1933), 2042(1933), 2042(1933), 2079(0)
<b>11-1</b>	<b>1855(894), 1876(679), 1895(38)</b> , 1975(384), 2004(55), 2005(130), 2012(66), 2025(2575), 2038(1475), 2046(1117), 2073(109)
<b>11-2</b>	<b>1659(189), 1875(289), 1876(462)</b> , 1996(160), 1998(1), 2004(669), 2010(629), 2030(872), 2033(1984), 2039(2152), 2067(12)

Infrared intensities in parentheses are in  $\text{km/mol}$  and bridging  $\nu(\text{CO})$  frequencies are in bold

**Table 2** Infrared  $\nu(\text{CO})$  vibrational frequencies ( $\text{cm}^{-1}$ ) predicted for all  $\text{Ir}_4(\text{CO})_{10}$  isomers

<b>10-1</b>	<b>1836(356)</b> , 1974(114), 1979(26), 1993(381), 1997(420), 2002(288), 2023(1047), 2028(2115), 2029(1945), 2063(44)
<b>10-3</b>	<b>1834(203), 1857(372)</b> , 1968(72), 1986(228), 1988(714), 2005(493), 2010(1661), 2021(2053), 2033(963), 2067(270)
<b>10-4</b>	1959(11), 1974(392), 1982(350), 1982(55), 2000(475), 2007(64), 2021(2299), 2026(1872), 2032(861), 2076(326)

Infrared intensities in parentheses are in  $\text{km/mol}$ ; bridging  $\nu(\text{CO})$  frequencies are in bold

The other structure found for  $\text{Ir}_4(\text{CO})_{11}$  (**11-2**) is a  $C_2$  symmetry minimum, lying 16.1 kcal/mol (BP86) or 19.9 kcal/mol (MPW1PW91) in energy above the global minimum **11-1**. Structure **11-2** has an interesting geometry, consisting of a butterfly array of iridium atoms with a unique  $\mu_4$ -CO group bridging all four metal atoms, two edge-bridging CO groups, and eight terminal CO groups (Fig. 3). An analogous structure is predicted to be the lowest energy structure of  $\text{Co}_4(\text{CO})_{11}$  [11]. The four outer edges of the  $\text{Ir}_4$  butterfly skeleton of **11-2** are predicted to be 2.749 and 2.801 Å (BP86) or 2.718 and 2.769 Å (MPW1PW91) whereas the unique edge corresponding to the “body” of the butterfly is predicted to be 2.793 Å (BP86) or 2.745 Å (MPW1PW91). All of these five Ir–Ir distances are reasonable for single bonds in accord with the butterfly structure. The long non-bonding Ir··Ir distance between the two wingtips of the butterfly is predicted to be 4.355 Å (MPW1PW91). The unique  $\mu_4$ -CO group bridging all four iridium atoms in **11-2** is slightly asymmetrical (Fig. 3) with two shorter Ir–C distances of 2.211 Å (BP86) or 2.169 Å (MPW1PW91) and two longer Ir–C distances of 2.302 Å (BP86) or 2.296 Å (MPW1PW91). This  $\mu_4$ -CO group is predicted to exhibit an unusually low  $\nu(\text{CO})$  frequency (Table 1), namely 1,659  $\text{cm}^{-1}$  (BP86), consistent with a very long C–O bond. For comparison, the  $\nu(\text{CO})$  frequency of the  $\mu_4$ -CO group in the analogous  $\text{Co}_4(\text{CO})_8(\mu\text{-CO})_2(\mu_4\text{-CO})$  structure (Fig. 2) is predicted to be 1,636  $\text{cm}^{-1}$  by the same method. In addition, the experimental  $\nu(\text{CO})$  frequency of the  $\mu_4$ -CO group in  $\text{Rh}_4(\text{CO})_4(\mu\text{-CO})_4(\text{PBu}_3^t)_2(\text{PtPBu}_3^t)(\mu_4\text{-CO})$  is reported [12] to be 1,704  $\text{cm}^{-1}$ . The Ir–C distances to the two edge-bridging CO groups in **11-2** are 2.069 Å and 2.102 Å (BP86) or 2.042 Å and 2.118 Å (MPW1PW91), and the corresponding  $\nu(\text{CO})$  frequencies are 1,875 and 1,876  $\text{cm}^{-1}$  (BP86), in a typical region for edge-bridging carbonyl groups.

### 3.1.3 $\text{Ir}_4(\text{CO})_{10}$

The global minimum predicted by the DFT methods is  $\text{Ir}_4(\text{CO})_{10}$  structure **10-1** (Fig. 4 and Table 2), which has a single bridging CO group exhibiting a  $\nu(\text{CO})$  frequency at 1,836  $\text{cm}^{-1}$  in the typical region for bridging carbonyls. Again, the MP2 method predicts the unbridged structure **10-2** to be global minimum, lying 5.7 kcal/mol in energy below **10-1**. In **10-1**, its six all non-equivalent Ir–Ir distances are predicted to be 2.676, 2.679, 2.698, 2.771, 2.776, and 2.867 Å (MPW1PW91). The longest Ir–Ir edge is the one bridged by the carbonyl group. All of these can be considered to be formal Ir–Ir single bonds, since the experimental distance for the Ir–Ir single bonds in the  $\text{Ir}_4(\text{CO})_{12}$  structure **12-2** is 2.693 Å. Optimization of an unbridged  $\text{Ir}_4(\text{CO})_{10}$  structure by the MPW1PW91 method led to the second  $\text{Ir}_4(\text{CO})_{10}$  structure **10-2** with all terminal carbonyls (Fig. 4). However, the BP86 method gave structure **10-1**.

Two higher energy  $\text{Ir}_4(\text{CO})_{10}$  structures were also found (Fig. 4). The  $C_s$  doubly bridged structure **10-3** lies 10.0 kcal/mol (BP86) or 12.7 kcal/mol (MPW1PW91) above the global minimum **10-1**. The bridging  $\nu(\text{CO})$  frequencies in **10-3** (Table 2) are predicted to be 1,834 and 1,857  $\text{cm}^{-1}$  in the typical bridging carbonyl region (Table 2). The two equivalent bridged Ir–Ir edges in **10-3** are 2.767 Å (BP86) or 2.731 Å (MPW1PW91), whereas the unbridged edges are 2.726, 2.768, and 2.934 Å (B3LYP) or 2.697, 2.724, and 2.955 Å (MPW1PW91). The other  $C_s$  symmetry  $\text{Ir}_4(\text{CO})_{10}$  structure **10-4** with all terminal carbonyls lies 12.7 kcal/mol (BP86) or 13.4 kcal/mol (MPW1PW91) in energy above the global minimum **10-1**. The lengths of the Ir–Ir bonds in **10-4** are predicted to be 2.647, 2.674, 2.705, and 2.716 Å (MPW1PW91).

**Table 3** Infrared  $\nu(\text{CO})$  vibrational frequencies ( $\text{cm}^{-1}$ ) predicted for the four  $\text{Ir}_4(\text{CO})_9$  structures

<b>9-1</b>	<b>1838(420)</b> , 1967(249), 1983(302), 1987(324), 1995(26), 2009(2526), 2015(1567), 2029(1031), 2059(256)
<b>9-2</b>	<b>1841(621)</b> , 1975(259), 1975(6), 1999(111), 2000(292), 2018(1500), 2021(2972), 2026(1241), 2062(135)
<b>9-3</b>	<b>1825(559)</b> , <b>1862(551)</b> , 1976(11), 1980(122), 2006(276), 2012(2440), 2027(882), 2028(1989), 2062(295)

Infrared intensities in parentheses are in  $\text{km/mol}$ ; bridging  $\nu(\text{CO})$  frequencies in bold

**Table 4** Infrared  $\nu(\text{CO})$  vibrational frequencies ( $\text{cm}^{-1}$ ) predicted for the five  $\text{Ir}_4(\text{CO})_8$  structures

<b>8-1</b>	1961(252), 1976(263), 1983(353), 1987(41), 2003(2580), 2013(1482), 2026(1059), 2055(210)
<b>8-2</b>	<b>1841(445)</b> , 1972(82), 1982(751), 1990(243), 2000(1342), 2018(1848), 2026(1127), 2056(239)
<b>8-3</b>	<b>1853(497)</b> , <b>1889(368)</b> , 1975(300), 1988(108), 2001(1717), 2016(1587), 2027(1288), 2056(249)
<b>8-4</b>	<b>1836(556)</b> , <b>1871(430)</b> , 1981(273), 1990(282), 1998(1279), 2008(1711), 2033(1118), 2056(447)
<b>8-5</b>	1970(18), 1978(588), 1987(648), 1989(165), 2012(2263), 2013(1775), 2028(941), 2056(168)

Infrared intensities in parentheses are in  $\text{km/mol}$ ; bridging  $\nu(\text{CO})$  frequencies are in bold

### 3.1.4 $\text{Ir}_4(\text{CO})_9$

Three  $\text{Ir}_4(\text{CO})_9$  structures were obtained by the BP86 method (Fig. 5). The global minimum structure **9-1**, with  $C_1$  symmetry, has a single bridging carbonyl group, which is predicted to exhibit a  $\nu(\text{CO})$  frequency at  $1,838 \text{ cm}^{-1}$  in the typical region for bridging CO groups (Table 3). A higher energy  $\text{Ir}_4(\text{CO})_9$  structure **9-2** also has a single bridging CO group and lies 8.0 kcal/mol (MPW1PW91) or 6.9 kcal/mol (BP86) above **9-1**. However, the MP2 method predicts a lower energy for **9-2**, lying 17.0 kcal/mol below **9-1**. This structure exhibits one (MPW1PW91) or two (BP86) small imaginary vibrational frequencies. Following the corresponding normal modes collapses **9-2** to the global minimum **9-1**. A higher energy doubly bridged  $C_s$   $\text{Ir}_4(\text{CO})_9$  structure **9-3** lies 8.4 kcal/mol (BP86) or 10.4 kcal/mol (MPW1PW91) above the global minimum **9-1** with an imaginary vibrational frequency of  $62i \text{ cm}^{-1}$  (BP86) or  $65i \text{ cm}^{-1}$  (MPW1PW91). The bridging carbonyl groups in **9-3** are predicted to exhibit  $\nu(\text{CO})$  frequencies at 1,825 and  $1,862 \text{ cm}^{-1}$  (Table 3).

A fourth  $\text{Ir}_4(\text{CO})_9$  structure **9-4** (Fig. 5) was also found using the MPW1PW91 method. This structure collapses to **9-1** when the BP86 method is used. Structure **9-4** has all terminal CO groups and a butterfly arrangement of the four iridium atoms with only five Ir–Ir bonding distances, namely 2.644, 2.653, 2.669, 2.719, and 2.721 Å. The sixth Ir...Ir distance of 3.921 Å corresponds to the distance between the wingtips of the butterfly and is far too long to be considered as a bonding distance.

### 3.1.5 $\text{Ir}_4(\text{CO})_8$

Five structures were optimized for  $\text{Ir}_4(\text{CO})_8$  (Fig. 6). The first two  $\text{Ir}_4(\text{CO})_8$  structures **8-1** and **8-2** are  $C_1$  symmetry structures with tetrahedral  $\text{Ir}_4$  frameworks and have no

imaginary vibrational frequencies. They are essentially degenerate, with structure **8-2** lying only 1.1 kcal/mol (BP86) or 0.1 kcal/mol (MPW1PW91) above **8-1**. The MP2 method predicts the unbridged structure **8-1** to lie 8.0 kcal/mol in energy below the singly-bridged structure **8-2**. These two structures differ in that **8-2** has a bridging CO group whereas structure **8-1** has all terminal CO groups. The  $\nu(\text{CO})$  frequency for the bridging carbonyl group in **8-2** is predicted to be  $1,841 \text{ cm}^{-1}$  (BP86) (Table 4).

The next  $\text{Ir}_4(\text{CO})_8$  structure **8-3** has  $C_s$  symmetry and lies 2.6 kcal/mol (BP86 and MPW1PW91) in energy above the global minimum **8-1** (Fig. 6). Structure **8-3** has a small imaginary vibrational frequency at  $26i \text{ cm}^{-1}$ . Following the corresponding normal mode leads to the global minimum **8-1**. The following  $\text{Ir}_4(\text{CO})_8$  structure **8-4** has  $C_1$  symmetry with only terminal carbonyl groups and lies 4.0 kcal/mol (BP86) or 6.2 kcal/mol (MPW1PW91) above the global minimum **8-1**. The  $C_s$  structure **8-5** for  $\text{Ir}_4(\text{CO})_8$  with all terminal carbonyl groups is predicted to have a small imaginary vibrational frequency at  $93i \text{ cm}^{-1}$  (BP86) or  $77i \text{ cm}^{-1}$  (B3LYP). Following the corresponding normal mode leads to the  $C_1$  structure **8-2**.

### 3.2 Iridium–iridium distances

Table 5 summarizes the Ir–Ir distances for all of the  $\text{Ir}_4(\text{CO})_n$  structures discussed in this paper. In the species with  $\text{Ir}_4$  tetrahedra, which correspond to most of the structures discussed in this paper, these Ir–Ir distances fall in the narrow range 2.6–2.8 Å, with very few Ir–Ir distances outside this range. This range can be taken to correspond to formal single bonds in a tetrahedral  $\text{Ir}_4$  structure, given that 2.693 Å is the experimental bond distance for **12-2**. No clear examples of shorter Ir–Ir bonds were observed corresponding to distinct double or triple bonds

**Table 5** The six Ir–Ir distances in the  $\text{Ir}_4(\text{CO})_n$  ( $n = 12, 11, 10, 9, 8$ ) structures (Å) predicted by the MPW1PW91/SDD method

$\text{Ir}_4(\text{CO})_{12}$							
<b>12-1</b> ( $C_{3v}$ )	2.743	2.743	2.743	2.780	2.780	2.780	2.780
<b>12-2</b> ( $T_d$ )	2.720	2.720	2.720	2.720	2.720	2.720	2.720
$\text{Ir}_4(\text{CO})_{11}$							
<b>11-1</b> ( $C_s$ )	2.710	2.710	2.721	2.758	2.758	2.811	2.811
<b>11-2</b> ( $C_2$ )	2.718	2.718	2.745	2.769	2.769	4.355	4.355
$\text{Ir}_4(\text{CO})_{10}$							
<b>10-1</b> ( $C_1$ )	2.676	2.679	2.698	2.771	2.776	2.867	2.867
<b>10-2</b> ( $C_1$ )	2.665	2.690	2.694	2.700	2.714	2.726	2.726
<b>10-3</b> ( $C_s$ )	2.697	2.697	2.724	2.731	2.731	2.955	2.955
<b>10-4</b> ( $C_s$ )	2.647	2.647	2.674	2.705	2.705	2.716	2.716
$\text{Ir}_4(\text{CO})_9$							
<b>9-1</b> ( $C_1$ )	2.646	2.664	2.669	2.694	2.756	2.891	2.891
<b>9-2</b> ( $C_2$ )	2.647	2.647	2.769	2.799	2.799	2.867	2.867
<b>9-3</b> ( $C_s$ )	2.652	2.711	2.711	2.800	2.800	2.883	2.883
<b>9-4</b> ( $C_1$ )	2.644	2.653	2.669	2.719	2.721	3.921	3.921
$\text{Ir}_4(\text{CO})_8$							
<b>8-1</b> ( $C_1$ )	2.603	2.643	2.649	2.672	2.677	2.686	2.686
<b>8-2</b> ( $C_1$ )	2.599	2.600	2.702	2.719	2.784	2.798	2.798
<b>8-3</b> ( $C_s$ )	2.605	2.605	2.689	2.723	2.723	2.855	2.855
<b>8-4</b> ( $C_1$ )	2.585	2.639	2.671	2.696	2.753	2.845	2.845
<b>8-5</b> ( $C_s$ )	2.540	2.623	2.623	2.682	2.761	2.761	2.761

The long non-bonding Ir...Ir distances in the butterfly structures **11-2** and **9-4** are in *italics*

required to give the iridium atoms the favored 18-electron configuration [37, 38]. This suggests that the effective iridium configurations in many of the unsaturated  $\text{Ir}_4(\text{CO})_n$  ( $n = 11, 10, 9$ , and 8) derivatives are less than the favored 18-electron configuration. This is consistent with the spherical aromaticity [39, 40] of a tetrahedral system, which is likely to delocalize the bond shortening corresponding to metal–metal multiple bonds in an unsaturated system among all of the available bonds of a suitable type. This is analogous to the lack of distinct carbon–carbon single and double bonds in the structure of benzene. In this connection note that  $\text{Ir}_4(\text{CO})_{12}$  is isovalent with the tetrahedral molecule  $\text{P}_4$ , which is the prototypical tetrahedral molecule exhibiting spherical aromaticity.

In the many  $\text{Ir}_4(\text{CO})_n$  species in Table 5 with a central  $\text{Ir}_4$  tetrahedron, all six tetrahedral edges are within a reasonable bonding distance, typically the 2.6–2.8 Å range mentioned above. The Wiberg Bond Indices [41] of unbridged Ir–Ir edges of this type fall in the range 0.40–0.63 whereas those of the singly carbonyl-bridged Ir–Ir edges are lower in the range 0.29–0.38. Two species with  $\text{Ir}_4$  butterflies were found in this work, namely the  $\text{Ir}_4(\text{CO})_{11}$  structure **11-2** and the  $\text{Ir}_4(\text{CO})_9$  structure **9-4**. Such structures have one long non-bonding Ir...Ir distance of  $\sim 4$  Å, corresponding to the distance between the wingtips of the butterfly. The Wiberg Bond Index for this non-bonding Ir...Ir interaction is very small at  $\sim 0.05$ .

### 3.3 Dissociation energies

Table 6 summarizes the carbonyl dissociation energies for the reactions  $\text{Ir}_4(\text{CO})_n \rightarrow \text{Ir}_4(\text{CO})_{n-1} + \text{CO}$  based on the lowest energy structures. All of these CO dissociation energies are greater than 30 kcal/mol suggesting that at least the low energy structures reported in this paper might be possible synthetic targets or at least molecules that could be observed in low temperature matrix photolyses. Furthermore, the predicted dissociation energies reported in Table 6 for the iridium carbonyl derivatives are very similar to the experimental carbonyl dissociation energies for  $\text{Ni}(\text{CO})_4$ ,  $\text{Fe}(\text{CO})_5$ , and  $\text{Cr}(\text{CO})_6$  of 27, 41, and 37 kcal/mol, respectively [42].

**Table 6** Dissociation energies (kcal/mol) for the successive removal of CO groups from  $\text{Ir}_4(\text{CO})_{12}$ 

	BP86/SDD	MPW1PW91/SDD
$\text{Ir}_4(\text{CO})_{12} \rightarrow \text{Ir}_4(\text{CO})_{11} + \text{CO}$	40.9	41.3
$\text{Ir}_4(\text{CO})_{11} \rightarrow \text{Ir}_4(\text{CO})_{10} + \text{CO}$	39.5	40.0
$\text{Ir}_4(\text{CO})_{10} \rightarrow \text{Ir}_4(\text{CO})_9 + \text{CO}$	37.1	42.7
$\text{Ir}_4(\text{CO})_9 \rightarrow \text{Ir}_4(\text{CO})_8 + \text{CO}$	36.2	30.1

All results reported refer to the lowest energy structures of  $\text{Ir}_4(\text{CO})_n$

**Acknowledgments** We are indebted to the Scientific Research Fund of State Key Laboratory of Explosion Science and Technology (2DKT10-01a) and the Research Fund for the Doctoral Program of Higher Education (20104407110007) of China as well as the U. S. National Science Foundation (Grants CHE-0716718 and CHE-1054286) for support of this research.

## References

- Hieber W, Lagally HZ (1940) *Anorg Chem* 245:321
- Chaston SHH, Stone FGA (1969) *J Chem Soc A*, 500
- Whyman R (1972) *J Chem Soc Dalton* 2294
- Malatesta L, Caglio G, Angoletta M (1972) *Inorg Syn* 13:95
- Stuntz GF, Shapley JR (1976) *Inorg Nucl Chem Lett* 12:49
- Churchill MR, Hutchinson JP (1978) *Inorg Chem* 17:3528
- Wei CH, Dahl LFJ (1966) *Am Chem Soc* 88:1821
- Wei CH (1969) *Inorg Chem* 8:2384
- Farrugia LJJ (2000) *Cluster Sci* 11:39
- Dahlinger K, Falcone F, Poë AJ (1986) *Inorg Chem* 25:2654
- Zhang X, Li Q-s, Xie Y, King RB, Schaefer HF (2008) *Eur J Inorg Chem*, 2158
- Adams RD, Captain B, Pellechiaq PJ, Smith JL (2004) *Inorg Chem* 43:2695
- Li Q-s, Xu B, Xie Y, King RB, Schaefer HF (2007) *Dalton Trans* 4312
- Xu B, Li Q-S, Xie Y, King RB, Schaefer HF (2008) *Dalton Trans*, 1366
- Ehlers AW, Frenking GJ (1994) *Am Chem Soc* 116:1514
- Li J, Schreckenbach G, Ziegler TJ (1995) *Am Chem Soc* 117:486
- Jonas V, Thiel WJ (1995) *Chem Phys* 102:8474
- Brynda M, Gagliardi L, Wimark PO, Power PP, Roos BO (2006) *Angew Chem Int Ed* 45:3804
- Zhao Y, Truhlar DG (2006) *J Chem Phys* 124: 224105
- Niu S, Hall MB (2000) *Chem Rev* 100:353
- Buhl M, Kabrede H (2006) *J Chem Theory Comput* 2:1282
- Becke AD (1988) *Phys Rev A* 38:3098
- Perdew JP (1986) *Phys Rev B* 33:8822
- Adamo C, Barone VJ (1998) *Chem Phys* 108:664
- Feng X, Gu J, Xie Y, King RB, Schaefer HFJ (2007) *Chem Theory Comput* 3:1580
- Møller C, Plesset MS (1934) *Phys Rev* 46:618
- Pople JA, Binkley JS, Seeger R (1976) *Int J Quantum Chem Symp* 10:1
- Andrae D, Haussermann U, Dolg M, Stoll H, Preuss H (1990) *Theor Chim Acta* 77:123
- Bergner A, Dolg M, Kuechle W, Stoll H, Preuss H (1993) *Mol Phys* 80:1431
- Dunning THJ (1970) *Chem Phys* 53:2823
- Huzinaga SJ (1965) *Chem Phys* 42:1293
- Frisch MJ et al. (2004) *Gaussian 03, Revision C 02*; Gaussian, Inc.; Wallingford CT (see Supporting Information for details)
- Papas BN, Schaefer HFJ (2006) *Mol Struct* 768:175
- Silaghi-Dumitrescu I, Bitterwolf TE, King RBJ (2006) *Am Chem Soc* 128:5342
- Jonas V, Thiel W (1995) *J Chem Phys* 102:8474
- Wei CH, Wilkes GR, Dahl LFJ (1967) *Am Chem Soc* 89:4792
- Hartwig J (2009) *Organotransition metal chemistry: from bonding to catalysis*. University Science Books, Sausalito, CA
- Crabtree RH (2009) *The organometallic chemistry of the transition metals*, 5th edn. Wiley, New York, pp 25–32
- Hirsch A, Chen Z, Jiao H (2001) *Angew Chem Int Ed* 40:2834
- Chen Z, King RB (2005) *Chem Rev* 105:3613
- Weinhold F, Landis CR, Valency Bonding (2005) *A natural bond order donor-acceptor perspective*. Cambridge University Press, Cambridge
- Sunderlin LS, Wang D, Squires RRJ (1993) *Am Chem Soc* 115:12060